

# Confined Growth of Poly(butylene succinate) in Its Miscible Blends with Poly(vinylidene fluoride): Morphology and Growth Kinetics

Tianchang Wang,<sup>†</sup> Huihui Li,<sup>‡</sup> Feng Wang,<sup>‡</sup> Shouke Yan,<sup>\*,†,‡</sup> and Jerold M. Schultz<sup>\*,§</sup>

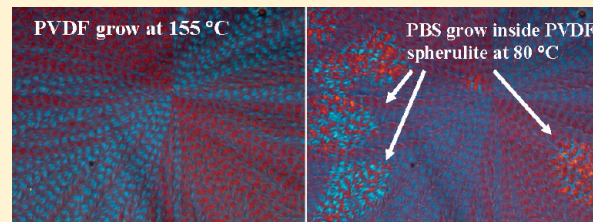
<sup>†</sup>State Key Laboratory of Polymer Physics and Chemistry, Institute of Chemistry, The Chinese Academy of Sciences, Beijing 100190, P. R. China

<sup>‡</sup>State Key Laboratory of Chemical Resource Engineering, Beijing University of Chemical Technology, Beijing 100029, P. R. China

<sup>§</sup>Department of Materials Science and Engineering, University of Delaware, Newark, Delaware 19716, United States

Supporting Information

**ABSTRACT:** The morphology and confined crystallization behavior of poly(butylene succinate) (PBS) in miscible poly(vinylidene fluoride) (PVDF)/PBS blends has been studied using differential scanning calorimetry (DSC) and optical and atomic force microscopy (OM and AFM). It was found that PBS crystal lamellae nucleated and grew confined inside the matrix of PVDF spherulites. Crystallized PBS domains grow with an ellipsoidal outline within PVDF spherulites formed at a relatively high PVDF crystallization temperature ( $T_{c,PVDF}$ ), while circular domains, engulfing several PVDF spherulites, are seen when growing in the PVDF spherulites created at lower  $T_{c,PVDF}$ . The growth kinetics of PBS confined in the PVDF matrix was investigated under various conditions. The growth rate of PBS ( $G_{PBS}$ ) increases with decreasing crystallization temperature and increasing PBS content under a given PVDF crystallization temperature ( $T_{c,PVDF}$ ). For  $T_{c,PVDF}$  above 145 °C,  $G_{PBS}$  decreases with  $T_{c,PVDF}$  for both 50:50 and 30:70 PVDF/PBS blends. However, for  $T_{c,PVDF}$  below 145 °C, 50:50 and 30:70 PVDF/PBS blends exhibit the opposite  $G_{PBS}$  trend; that is,  $G_{PBS}$  for the 50:50 blend decreases with decreasing  $T_{c,PVDF}$ , while for the 30:70 PVDF/PBS blend  $G_{PBS}$  increases with decreasing  $T_{c,PVDF}$ . It is shown that this behavior cannot be associated with the effect of crossing the boundary of smaller PVDF spherulites formed at a lower temperature. Rather, the behavior appears to be related to the interleaving growth of PBS lamellae among PVDF lamellae or between bundles of PVDF lamellae (fibrils), as in situ AFM observation shows. It is found that the interconnectedness of the molten pockets within the PVDF spherulites, which depends on the PVDF crystallization temperature, is an important factor determining the growth kinetics of PBS confined within the PVDF scaffold.



## 1. INTRODUCTION

It is well-known that the properties of polymeric materials depend strongly on their supermolecular structures and morphologies. Therefore, blending one polymer with another offers a simple and economical way for producing new polymeric materials with desired properties. These blends can be miscible or immiscible systems, including amorphous/amorphous and amorphous/crystalline, as well as crystalline/crystalline components. Among all of these possible blends, miscible crystalline/crystalline polymer blends exhibit a wide variety of morphologies and crystal structures, depending on the blend ratio and thermal conditions.<sup>1–3</sup> The crystallization behavior and related morphological control of such blend systems have consequently been a subject of continuing interest in both academia and industry.

For miscible crystalline/crystalline blends, it is well-documented that a factor influencing the crystallization kinetics and morphology is the difference in the melting points ( $T_m$ ) of the two components, for binary miscible crystalline/crystalline blends crystallizing from the homogeneous melt.<sup>4–6</sup> When the difference in  $T_m$  is small enough, both constituents can crystallize simultaneously and form interpenetrated spherulites. That is, the

spherulites of one component continue to grow within the spherulites of the other component after they come in contact.<sup>7–13</sup> When the difference in  $T_m$  is of an intermediate value, typically 50–70 K, two-step crystallization occurs. In this case, during cooling or during isothermal crystallization above the melting point of the lower melting component, the high- $T_m$  component crystallizes first and its spherulites fill the whole volume (given a sufficiently low diffusion length). Lamellar crystals of the other component then nucleate and grow inside the confined space within the spherulites of the pre-existing high- $T_m$  component (interfilling crystallization),<sup>14–17</sup> maintaining the original spherulitic shape.<sup>18–21</sup>

It should be pointed out that the crystallization and morphology development of binary miscible crystalline polymer blends are far from having a full understanding. Moreover, until now, much more attention has been paid to the crystallization kinetics and morphology of the high- $T_m$  component in miscible

**Received:** April 20, 2011

**Revised:** May 16, 2011

**Published:** May 19, 2011

crystalline/crystalline polymer blends. There has been significantly little study of the morphology and confined growth behavior of the low- $T_m$  component in the matrix of the high- $T_m$  component. This rests on the fact that observation of the growth of the low- $T_m$  component is usually difficult in crystalline/crystalline polymer blends, due to the existence of previously formed crystals of the high- $T_m$  component. In most cases, only tiny crystals of the low- $T_m$  component can grow within the molten pockets contained within the pre-existing spherulites or at the boundaries of the spherulites of the high- $T_m$  component. The crystallization of the low- $T_m$  component should be, however, of interest, as it is affected not only by blend composition and crystallization conditions, but also strongly by the pre-existing crystal framework of the high- $T_m$  component in the blends. Lee et al.<sup>18</sup> have studied the miscibility and crystallization of poly(vinylidene fluoride)/poly(butylene succinate) (PVDF/PBS) blends. Through optical microscopy observation, they found that the crystal morphology of PBS was influenced strongly by the presence of pre-existing spherulitic PVDF crystals developed under different crystallization conditions. A recent study on the crystallization behavior of PBSA in the PVDF matrix performed by Qiu et al.<sup>22</sup> found also that the crystal growth rate of the PBSA was strongly affected by the PVDF composition. They concluded that the physical constraints imposed by the previously crystallized PVDF might contribute to the decrease in PBSA crystallization rate. For this aspect, Ikehara et al.<sup>23</sup> have investigated the effect of previously formed PBS spherulites on the details of spherulitic growth of poly(ethylene oxide) (PEO). They report that, when PEO crystallizes in PBS spherulites grown below 80 °C, the PEO growth rate increases with the crystallization temperature of the PBS but decreases with increasing PBS crystallization temperature when PBS is crystallized above 80 °C. They show that the crossing of PBS boundaries provides a hindrance to the growth of PEO lamellae and propose this spherulite boundary hindrance as a chief cause of the reversal of the kinetics. Since they show clear evidence of the PEO growth front being held up before crossing PBS spherulite boundaries, this is a reasonable conclusion. There was, however, no detailed morphological evidence, particularly at the lamellar scale, related to the growth process of the low- $T_m$  component in the matrix of the pre-existing high- $T_m$  component. This detail can be resolved by scanning probe microscopy, which provides the necessary resolution to permit in situ study of the crystallization of the low- $T_m$  component within spherulites of the high- $T_m$  component. Moreover, it is not clear whether the phenomenon observed by Ikehara et al.<sup>23</sup> is universal to other polymer blend systems or not. We will show that for the PVDF/PBS system the proposed model cannot explain our kinetic results.

PVDF and PBS are both crystalline polymers, with a melting point gap of about 60 K and good miscibility.<sup>18</sup> Most important, the PVDF crystals are not a strong nucleant for PBS crystals. Because of this, PBS nucleates and grows relatively slowly within the scaffold of a PVDF spherulite, and it is possible to observe and identify the nucleation and growth behavior of PBS in the PVDF matrix. Therefore, in the present paper, PVDF and PBS have been chosen for detailed morphological characterization of the confined growth behavior of PBS in the spherulitic matrix of PVDF under various blend ratios and isothermal crystallization conditions. Observations under both polarized light and atomic force microscopy (AFM) have proved useful in defining the phenomenon of PBS crystallization. The kinetic study shows that the growth rates of PBS ( $G_{PBS}$ ) in 50:50 and 30:70 PVDF/PBS

blends exhibit different trends with the PVDF crystallization temperature ( $T_c$ <sub>PVDF</sub>). For the 50:50 blend,  $G_{PBS}$  increases with increasing  $T_c$ <sub>PVDF</sub> when  $T_c$ <sub>PVDF</sub> is below 145 °C but decreases with increasing  $T_c$ <sub>PVDF</sub> when  $T_c$ <sub>PVDF</sub> is above 145 °C.  $G_{PBS}$  for the 30:70 PVDF/PBS blend, however, decreases monotonically with increasing  $T_c$ <sub>PVDF</sub>. It will be shown that this result cannot be associated with the effect of crossing the boundary of smaller PVDF spherulites formed at lower temperature, as reported by Ikehara et al.<sup>23</sup> This unusual kinetics of PBS crystal growth within the PVDF spherulitic matrix is presented and discussed in Section 3.2. Morphological evidence for the differences in PBS growth behavior under different growth environments are given by in situ AFM observation in Section 3.3. These results show interleaving growth of PBS lamellae among PVDF lamellae or between bundles of PVDF lamellae (fibrils). The interconnectedness of the molten pockets within the PVDF spherulites, which depends on the PVDF crystallization temperature, is found to be an important factor determining the growth kinetics of PBS confined in the PVDF crystals.

## 2. EXPERIMENTAL SECTION

**2.1. Materials.** PVDF and PBS used in this work were purchased from Sigma-Aldrich Company and have a weight-average molecular weight of about  $2.7 \times 10^5$  g/mol and  $6.3 \times 10^4$  g/mol, respectively, measured by gel permeation chromatography (GPC) with eluents of *N,N*-dimethyl formamide (DMF) and chloroform, respectively. The melting points were measured to be 180 °C for PVDF and 120 °C for PBS. Both of them were used as received.

**2.2. Sample Preparation.** Blends of PVDF and PBS were prepared by solution blending. Both of them were dissolved in DMF, which serves as a common solvent, with desired mass proportions (total polymer concentration was 10 mg/mL). Thin films for optical microscopy (OM) and AFM observations were prepared by solution casting and spin-coating on glass slides, respectively. These films were allowed to dry under vacuum at 50 °C for 2 days. The thicknesses of the resultant films were estimated to be 10 μm for OM observation and 600 nm for AFM measurement. The obtained films were heat-treated at temperatures 30 °C above the melting point ( $T_m$ ) of the high- $T_m$  component for 3 min to erase the thermal history of the samples and were subsequently cooled to predetermined isothermal crystallization temperatures at about 80 °C/min for sufficient long times to ensure complete crystallization.

**2.3. Characterizations.** An Olympus BH-2 microscope equipped with a Linkam LK-600PM temperature controller was used in this study to observe the crystalline morphology. All of the optical micrographs shown in this paper were taken under crossed polarizers. Tapping-mode AFM images were obtained in the repulsive force region using a NanoScope III MultiMode AFM (Digital Instruments) equipped with a high-temperature heater accessory (Digital Instruments). Si cantilever tips (TESP) with a resonance frequency of approximately 300 kHz and a spring constant of about 40 N/m were used. The scan rates varied from 0.7 to 1.5 Hz. The scanning density was 512 lines/frame. The set-point amplitude ratio,  $A_{sp}/A_o$ , was adjusted to 0.6–0.9, where  $A_{sp}$  is the set-point amplitude and  $A_o$  is the amplitude of the free oscillation. The scanning time for each image is about 3 min, and the interval between two scans is about 9 min. DSC measurements for obtaining crystallinity values were carried out using a Perkin-Elmer Diamond DSC instrument with

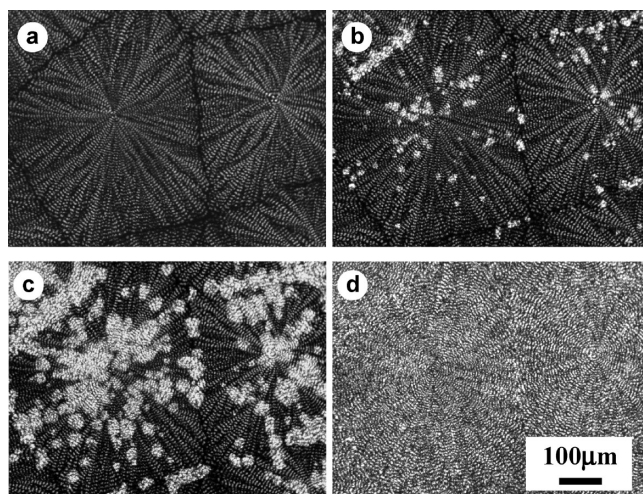


**Figure 1.** Optical micrographs of a 50:50 PVDF/PBS blend (a) crystallized first at 155 °C and then quenched to 80 °C for (b) 0.5 min, (c) 1.5 min, and (d) 20 min (completion of PBS crystallization), which present the nucleation and growth processes of PBS in PVDF matrix after quenching.

a liquid-nitrogen cooling accessory. Dry helium gas with a flow rate of 20 mL/min was purged through the DSC cell. The temperature and the heat flow of the equipment were calibrated with indium. Heating scans were initiated at the PVDF crystallization temperature, rather than at room temperature, to avoid additional crystallization upon cooling.

### 3. RESULTS AND DISCUSSION

**3.1. Morphology.** The morphology of PVDF in a 50:50 PVDF/PBS blend crystallized at 155 °C is displayed in Figure 1. Large spherulites of hundreds of micrometers in diameter were observed after complete crystallization of PVDF (see Figure 1a), while PBS was still molten. The spherulites are well-organized with ring-banded structures. The crystallization of PVDF corresponds to the transition from the fully amorphous to the semicrystalline state. In comparison with neat PVDF spherulites crystallized at the same temperature (see Figure S1 in the Supporting Information), the PVDF spherulites created in the 50:50 blend exhibit nonsmooth-linear boundaries. They exhibit also a larger spherulite size due to the low nucleation density after blending (ca. 340 μm for blend vs 160 μm for neat PVDF) and larger band periodicity (ca. 7.0 μm for blend vs 1.7 μm for neat PVDF). Most of these changes in morphological detail, relative to neat PVDF, reflect the reduced equilibrium melting point of PVDF in the blend (ca. 178 °C for the 50:50 blend, which is more than 10 °C lower than that of the neat PVDF) and the consequently lower undercooling. Following crystallization of the PVDF component, the blend is cooled rapidly to 80 °C, where the PBS component crystallizes isothermally. Several crystallized PBS domains were found to nucleate and grow continuously within the pre-existing PVDF spherulites until the domains impinge on each other (see Figure 1b–d). These small domains were confirmed to be PBS, as they melted at about 120 °C, while darker banded PVDF spherulites still existed. The brightness of the PVDF spherulites increases in the region where PBS has crystallized and remains unchanged in the area not yet reached by the PBS growth front. It should be pointed out that

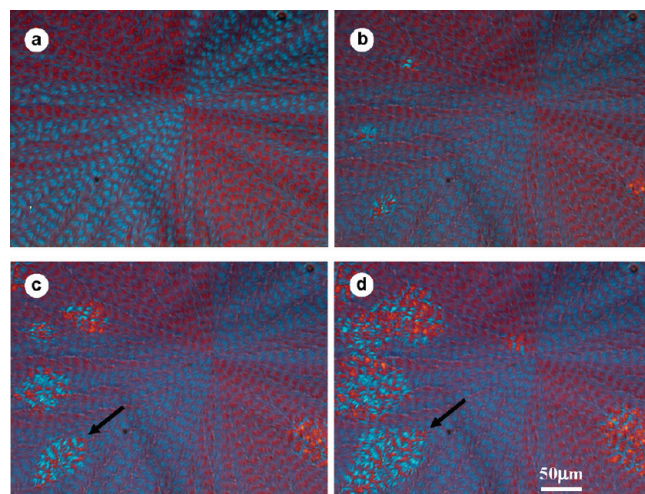


**Figure 2.** Enlarged optical micrographs show the nucleation and growth process of PBS in Figure 1. The black arrows in c and d indicate the crystallized PBS domains with ellipsoidal growth boundary.

the crystallization of PBS does not change the extinction feature of the pre-existing PVDF spherulites. This implies that PBS has crystallized with the lamellar crystals in the same orientation as the PVDF.

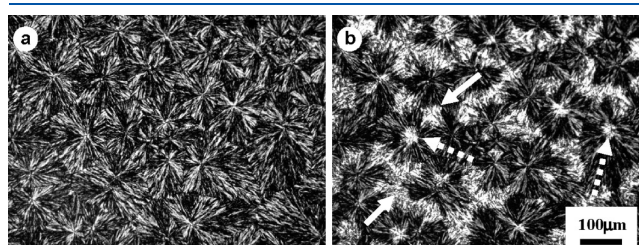
To better observe the growth process of PBS in PVDF spherulites, higher magnification optical micrographs are presented in Figure 2. As denoted by the arrows in Figure 2c and d, PBS exhibits an ellipsoidal growth outline whose long axis coincides with the radial direction of the PVDF spherulites. Since the PBS grows outward in all directions simultaneously in the PVDF matrix, the direction parallel to the radial direction of PVDF spherulite must have a larger growth rate than that perpendicular to it. This nonspherical growth habit further confirms that PBS indeed grows in the matrix of PVDF instead of forming a layered structure where the spherulites of both components merely superpose on each other as two separate layers. In the latter case, PBS spherulites should grow with circular boundaries because the subjacent PVDF lamellae do not influence the growth of PBS spherulites.

We also considered whether the PVDF has an epitaxial effect on the subsequent crystallization of PBS, which would greatly affect the morphology and crystallization behavior of the deposited polymer on the polymer substrate. By using the method of surface-induced crystallization on highly oriented polymer film,<sup>24</sup> no such effects have been found for PBS crystallized on the highly oriented PVDF film (see Figure S2 of the Supporting Information), which implies that PVDF has no epitaxial effect on the subsequent crystallization of PBS. It has been therefore considered that in the present case the ellipsoidal growth of PBS illustrates clearly the influence of pre-existing PVDF crystals on the growth behavior of the PBS crystals; that is, the orientation of PVDF lamellae affect the growth direction of PBS crystallized domains, as in the case of PBS/PEO system.<sup>23</sup>

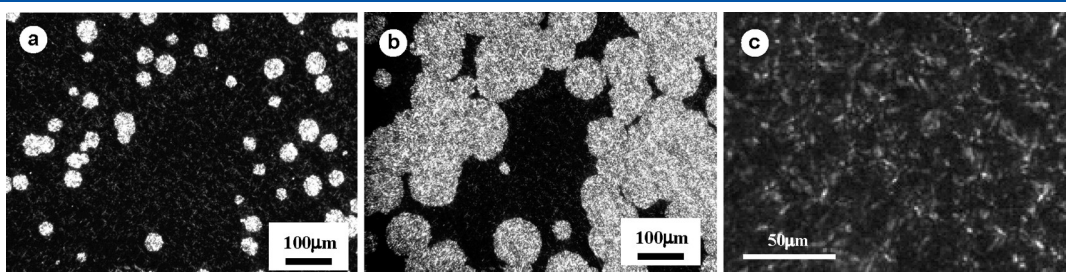
When PVDF is crystallized at lower temperatures, as shown for crystallization of a 50/50 blend at 145 °C in Figure 3a, one sees smaller spherulites without ring-banding. These spherulites are coarser and more open compared to neat PVDF, and the fibrils along the radial direction can be clearly seen. After cooling to 80 °C, PBS starts to nucleate and continues to grow in the PVDF matrix (see Figure 3b). One can also notice that here, just

as in the case of Figure 1, the sizes of the crystallized PBS domains are smaller than the PVDF spherulites, although the sizes of the PVDF spherulites and the PBS domains are more nearly comparable for this lower PVDF crystallization temperature. Nevertheless, a number of PBS domains have to nucleate within one larger PVDF spherulite. Moreover, in Figure 3b one can see that the crystallized PBS domains nucleate preferentially at the centers of the PVDF spherulites and at the interspherulite boundaries, as indicated by the dotted and solid arrows, respectively. Nucleation of the lower melting component at the centers of the higher melting component spherulites has been previously reported by Lu et al.<sup>25</sup> Very likely, the initial nucleation sites of the PVDF spherulites are also active for nucleating the subsequently crystallized PBS, resulting in the preferential nucleation of PBS spherulites at the centers of the PVDF spherulites. For the preferential nucleation of PBS at the intersections of PVDF spherulites, which is also seen in Figure 1b, this phenomenon rests on the higher concentration of PBS melt in the interspherulitic regions than in the intraspherulitic regions, due to the rejection of some portion of the PBS molecules into the melt at the growth fronts of PVDF spherulites during PVDF crystallization. This higher concentration of PBS between the spherulites should enhance the PBS nucleation rate in the interspherulitic regions of PVDF. It is seen that PBS grows radially outward from the centers of PVDF spherulites when nucleated at the centers of PVDF spherulites. Conversely, when nucleated at the spherulite boundary, PBS crystals grow backward toward the spherulite center until they impinge on the crystals coming from the center. These results show that the PVDF lamellae can still guide the growth of PBS crystals, as in the case of ring-banded PVDF matrix, although the lamellar organization may be less regular than that of the banded PVDF spherulites crystallized at 155 °C.

Figure 4 shows stages of the crystallization of PBS in a 50:50 blend at 80 °C, following the crystallization of PVDF at 130 °C. Figures 4a and b show the morphology after PBS crystallization for 1.5 and 4 min at 80 °C. Figure 4c is a blowup of a portion of



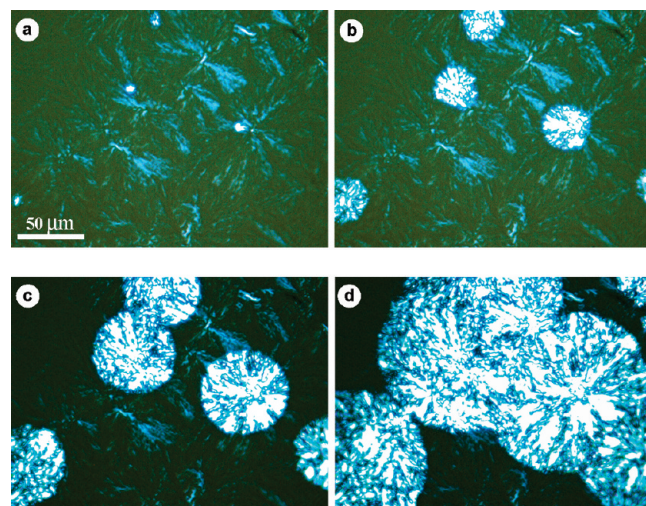
**Figure 3.** Optical micrographs of a 50:50 PVDF/PBS blend crystallized first at 145 °C (a) and then quenched to 80 °C and crystallizing PBS for 1 min (b).



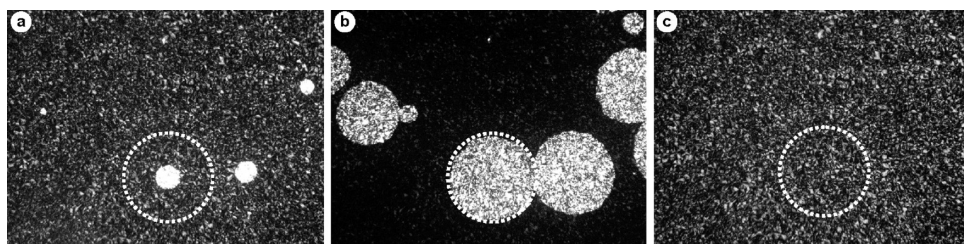
**Figure 4.** Optical micrographs of a 50:50 PVDF/PBS blend crystallized at 130 °C and subsequently quenched to 80 °C for (a) 1.5 min and (b) 4 min. (c) Enlargement of an area of a, with contrast and brightness adjusted to better reveal the PVDF crystal colonies.

Figure 4a, showing more clearly the fine scale of the PVDF spherulites (the white spots in the background). At 130 °C, densely nucleated spherulites of PVDF have formed, with a final size of approximately 10 μm. Cooling the sample from 130 to 80 °C, PBS crystallizes with strong birefringence against the darker PVDF matrix. The PBS nucleates randomly and growth occurs with a circular front, enveloping many small PVDF matrix spherulites (Figures 4a and b). Interestingly, these PBS crystallized domains keep their circular shape as they grow outward (see Figure 4b). In this case, the nucleation frequency of PBS crystallization is low enough that the spacing between the nucleated and growing PBS domains is much larger than the PVDF spherulites, requiring that the PBS domains grow through many PVDF spherulites. In this case, even if PBS domain grows more rapidly along the PVDF spherulite radial direction than along the tangential direction, the PBS domain grows through so many PVDF spherulites that its velocity of growth is averaged over many PVDF intraspherulite directions, and the envelope of the domain is circular.

Figure 5 parts a–d show, for the PVDF/PBS 30/70 blend, the stages of PBS crystallized domain growth at 80 °C, following PVDF crystallization at 130 °C. With one quantitative exception, these images are similar to what was seen for the 50:50 blend under the same conditions (Figure 4): roughly circular domains are seen, and these domains ultimately extend across PVDF spherulite boundaries. The difference relative to the 50:50 blend



**Figure 5.** Polarized optical micrographs of a 30:70 PVDF/PBS blend crystallized at 130 °C and subsequently quenched to 80 °C for (a) 2 min, (b) 3 min, (c) 4 min, and (d) 5.5 min. The contrast and brightness of the pictures have adjusted to better reveal the PVDF spherulites.



**Figure 6.** (a and b) Optical micrographs present the growth of PBS on the pre-existing PVDF matrix. (c) Micrograph of b after increasing to 120 °C to melt PBS. The dotted circles indicate the same position of the spherulite in b. PVDF crystals in the circular region of c are the same as in the circle of a after melting PBS, which implies no more PVDF crystals formed during the crystallization of PBS.

stems from the PVDF spherulite sizes. For the 30:70 blend, the size is approximately 50  $\mu\text{m}$ , some five times larger than for the 50:50 blend. This can be seen by comparing Figure 5a with Figure 4c, in both cases polarized light micrographs with the contrast and intensity changed so as to best reveal the PVDF spherulites. For the 30:70 blend, a PBS crystallized domain growing radially through a PVDF spherulite would cross at most one PVDF spherulite boundary before intercepting another PBS domain.

There is another issue to be addressed: is the increase of the birefringence intensity in Figures 4 and 5 caused only by the crystallization of PBS, or does PVDF also crystallize further during this process? This question is addressed in Figure 6. Figure 6 parts a and b show, for a 50:50 blend, two stages of PBS crystallized domain growth in PVDF crystallized at 130 °C, while Figure 6c shows the same field of view after melting the PBS. The matrix PVDF appears essentially the same in Figures 6a and c, showing that no further PVDF crystallization has occurred during the crystallization of PBS.

According to the results given above, several questions regarding to the morphological features of PBS should be discussed. The first question concerns the preferential sites of the PBS in the PVDF matrix. It is clear that the PBS crystallization most preferentially nucleated in the narrow regions between PVDF spherulites, seen in both Figures 1b and 3b. One can speculate on two possible causes. (i) It is likely that some portion of PBS has been rejected entirely from the growing PVDF spherulites and resides finally in the interspherulitic zones. The higher PBS concentration in those zones should effectively promote PBS crystal nucleation. One would expect this effect to increase with increasing  $T_{\text{c,PBS}}$  as the diffusion length increases with temperature. (ii) Another possibility is that stresses created in the melt because of the higher specific volume of crystals relative to the melt, could increase the driving force for PBS crystallization. However, while it is possible that such an effect can accelerate crystallization beyond a crystal growing freely in a melt,<sup>26</sup> Galeski and co-workers have shown that the stresses between spherulites create a negative pressure which slows crystallization.<sup>26–28</sup> Thus enrichment of PBS in the interspherulite region is most likely the correct explanation.

The second question relates to why the PBS crystallization sometimes preferentially nucleated at the centers of PVDF spherulites created at lower temperature. This behavior is shown in Figure 3. At the moment we cannot provide an exact answer for it. Nevertheless, it may originate from the fact that whatever effectively nucleated the PVDF spherulites was not expended in that event and was effective for PBS also.

Third, as for the nonspherical growth habit of PBS in the PVDF matrix, similar to the growth of PEO in the PBS matrix as

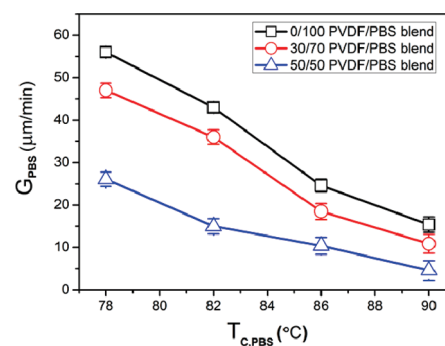


**Figure 7.** Dependence of the growth rate of PBS on the crystallization temperature and the blend ratio. The PVDF matrix crystallization temperature is fixed at 120 °C.

reported by Ikehara et al.,<sup>23</sup> it has been attributed to the differences in topological hindrance along different directions of the extended lamellae.

**3.2. Kinetics.** Since the pre-existing PVDF matrix has significantly influenced the morphology and growth behavior of PBS, especially for the 50:50 blend, it is useful to investigate the kinetics of the growth of PBS spherulites. Figure 7 shows the dependence of the spherulitic growth rate of PBS ( $G_{\text{PBS}}$ ) on the crystallization temperature ( $T_{\text{c,PBS}}$ ) and the blend ratio. To eliminate the effect of PVDF matrix on the growth of PBS, all of the growth rates were measured at a fixed PVDF crystallization temperature of 120 °C. The result is quantitatively a bit different from that reported previously,<sup>19</sup> which is attributed to the difference in PVDF crystallization temperature. Nonetheless, the variation trend of the PBS crystal growth rate has been clearly displayed. It is evident that the growth rate of PBS increases with decreasing crystallization temperature and with increasing PBS content in the blend at a given  $T_{\text{c,PBS}}$ . The composition dependence displayed here is reasonable, since the dilution effect should slow the growth rates of PBS in the blends.

Generally speaking, in addition to the blend ratio and crystallization temperature of PBS, the PVDF matrix crystallization temperature can also influence the growth of PBS in the confined environment. We focus here on the influences of the PVDF matrix crystallization temperature, together with the blend ratio, on the growth rates of PBS at a given PBS crystallization temperature. Figure 8 shows the variation of PBS growth rates at 85 °C as a function of blend ratio and crystallization temperature of the PVDF matrix. Each graphed point is the average values of repeated measurements. Above 145 °C, the PBS growth rate has been measured only along the radial direction; the tangential

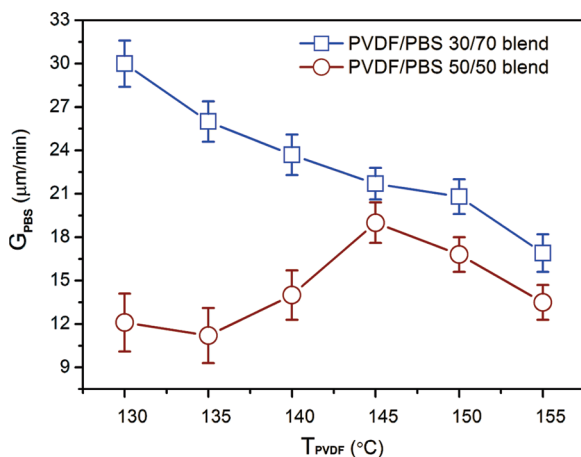


Figure 8. Variation of PBS growth rate at 85 °C as a function of blend ratio and crystallization temperature of the PVDF matrix.

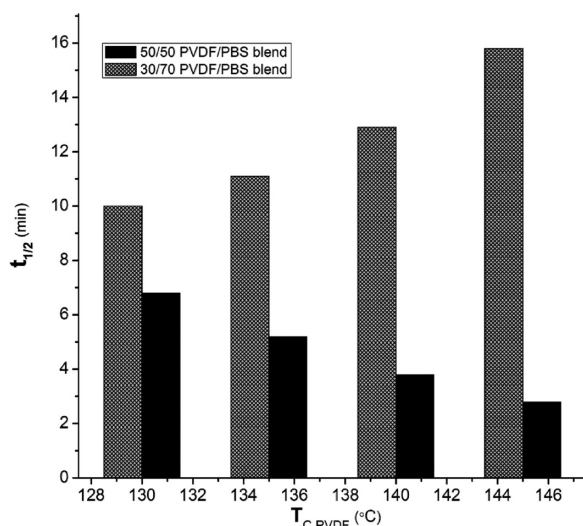


Figure 9. Half-time of PBS crystallized at 85 °C in the blend as a function of PVDF crystallization temperature and the blend ratio.

growth rate may be somewhat slower. For both blends in the studied temperature range, the PVDF/PBS 30:70 blend always exhibits a larger growth rate than the 50:50 blend at all  $T_{PVDF}$ . When the PVDF matrix is crystallized above 145 °C,  $G_{PBS}$  increases with decreasing  $T_{c,PVDF}$  for both blends. When the PVDF matrix is crystallized below 145 °C, very different behavior of the two blends is observed. For the 30:70 blend, the growth rate of PBS further increases with decreasing  $T_{PVDF}$ , while the PBS growth rate for the 50:50 blend decreases with further decreasing  $T_{PVDF}$ . A similar trend is also found in the half crystallization times ( $t_{1/2}$ ) for PBS in the blends as a function of  $T_{c,PVDF}$  and blend ratio, as shown in Figure 9. It is seen that, with  $T_{c,PVDF}$  below 146 °C, the  $t_{1/2}$  of PBS decreases with decreasing  $T_{c,PVDF}$  for the 30:70 blend but increases for the 50:50 blend. This trend agrees well with the data points presented in Figure 8 below 145 °C. It should be pointed out that the  $t_{1/2}$  values for the 30:70 blends are all larger than those for the 50:50 blends, indicating a slower crystallization of the 30:70 blends. The values of  $G_{PBS}$  for 30:70 blends are, however, larger than those for 50:50 blends. These results seem in contradiction. This is

actually caused by the fact that the  $t_{1/2}$  value depends not only on crystal growth rate but also on the induction time for nucleation as well as the nucleation density of the crystallized PBS domains. Taking this into account, the larger  $t_{1/2}$  for 30:70 PVDF/PBS blend compared to the 50:50 blend indicates that either the induction time for the crystallization of PBS in the 30:70 blend is longer than that in the 50:50 blend, or the nucleation density of the PBS in the 30:70 blend is lower than that in the 50:50 blend. Comparing Figure 4 with Figure 5, we do find that the nucleation of PBS in the 50:50 blend is somewhat earlier and denser than that in the 30:70 PVDF/PBS blend. The enhanced nucleation rate and efficiency of PBS, which is normally poor, in the 50:50 blend is possibly an effect of heterogeneous nucleation of PBS on existing PVDF crystals. That is, the larger spatial density of PVDF crystals in the blend provides a larger density of nucleation sites for PBS crystallization.

The above results clearly demonstrate that the PBS growth rate decreases monotonically with increasing  $T_{c,PVDF}$  for the 30:70 PVDF/PBS blend in the tested temperature range, while  $G_{PBS}$  increases first as  $T_{c,PVDF}$  is decreased from 155 to 145 °C but decreases and then remains sensibly constant as  $T_{c,PVDF}$  is decreased further for the 50:50 blend, as shown in Figure 8.

From these results, the different growth rate variation of PBS in different blends should be discussed here. To begin, a similar nonmonotonic growth rate dependence of PEO in the PBS/PEO blend on the crystallization temperature of PBS has been reported by Ikehara et al.<sup>23</sup> They have ascribed this aspect to a mismatch of the amorphous zones between the PBS spherulites, based on the fact that the PEO spherulite growth suspended at the boundary of PBS spherulites for about 10 s, and showed no distinct dependence on the blend composition and the crystallization temperature. Taking into account that the spherulite size of the PVDF in the 50:50 blend reduces tremendously with decreasing  $T_{c,PVDF}$ , the decrease of PBS crystal growth rate with a further decrease of the PVDF crystallization temperature, that is, lower than 145 °C, may be simply related to the boundary effect of the PVDF spherulites. This, however, cannot explain why the growth rate of PBS in the 30:70 PVDF/PBS blend decreases monotonically with  $T_{c,PVDF}$ , which is somewhat different from the PBS/PEO system where a nonmonotonic growth rate variation of PEO with  $T_{c,PEO}$  was obtained even for a 20:80 PBS/PEO blend. One may argue that the crystallizing PBS domains in the 30:70 PVDF/PBS blend are not much larger than the PVDF spherulites in the measured crystallization temperature range, such that a PBS domain would cross on average only one spherulite boundary, and that would likely not occur until late in the PBS growth period (see Figure 4). Therefore, the boundary of the PVDF spherulites shows no significant effect on the crystal growth kinetic of PBS. It should be pointed out that a monotonic decrease of the growth rate of PBS in the 30/70 PVDF/PBS blend with  $T_{c,PVDF}$  persists at much lower  $T_{c,PVDF}$ , for example, 90 °C, even though the formed PVDF spherulites at this temperature are much smaller than the growing PBS domains. The model of Ikehara et al. also cannot explain the decrease of growth rate of PBS in the 50:50 blend with a further increase of crystallization temperature of PVDF in the high temperature range, for example, from 145 to 155 °C, which should further increase the spherulite size of the PVDF, thereby reducing the incidence of spherulite boundary crossing. All of these phenomena indicate unambiguously that there are still other factors that influence the growth of PBS in the PVDF matrix.

**Table 1.** PVDF Crystallinity for Two PVDF/PBS Blends over the  $T_{c,\text{PVDF}}$  Range 130–155 °C

| blend composition | PVDF crystallization temperature (°C) |     |     |     |     |     |
|-------------------|---------------------------------------|-----|-----|-----|-----|-----|
|                   | 130                                   | 135 | 140 | 145 | 150 | 155 |
| 30:70             | 46%                                   | 46% | 46% | 52% | 45% | 37% |
| 50:50             | 49%                                   | 48% | 48% | 54% | 47% | 40% |

One may suggest that the local concentration of PBS may be an important factor influencing the growth rate of the PBS crystals. Regarding the local PBS concentration, one should recognize that, as PVDF crystallinity increases, the concentration of PVDF in the remaining melt decreases, thereby increasing the PBS concentration and facilitating PBS crystallization. However, as shown in Table 1, for both blends the PVDF crystallinity remains constant in the lower  $T_{c,\text{PVDF}}$  range and decreases with  $T_{c,\text{PVDF}}$  in the higher range. In neither  $T_{c,\text{PVDF}}$  range does the concentration of PBS decrease with  $T_{c,\text{PVDF}}$ , which would be necessary to explain the kinetic trend. Consequently, the effect of local PBS concentration can be ruled out.

Another factor which can influence the growth of PBS in the confined environment is the intrinsic morphological features of the pre-existing PVDF spherulites, for example, the number and distribution of molten pockets large enough to host the nucleation and growth of PBS lamellae at a thermodynamically stable thickness and the interconnectedness of the molten pockets. To disclose the effect of PVDF intraspherulitic morphological feature on the growth kinetics of the PBS, fine structures on a lamellar scale were monitored by AFM.

**3.3. AFM *In Situ* Studies of the Growth of PBS in PVDF Spherulites.** The development of PBS crystals within existing PVDF spherulites has been followed by *in situ* AFM. All of the AFM images selected below are typical and representative of the behavior for the conditions employed. Figure 10 presents the growth of PBS in a 50:50 blend with the PVDF matrix pre-crystallized at 140 °C. Figure 10a is scanned at 130 °C, and PBS is still molten at this temperature. A large quantity of PVDF edge-on lamellae with a small portion of flat-on lamellae can be seen. The lamellar organization, in this case, is quite regular. Long branched lamellae are oriented along the diagonal dominate. Generally, a spherulite grows by the radial propagation of stacks of lamellar crystals. These propagating lamellar stacks appear as long fibrils in optical microscopy and have been referred to variously as fibrils, growth arms, and lamellar bundles. The fibrils branch with some frequency. In the present case, as one can see in Figure 10a, the uncrossed pockets within the PVDF spherulite are of two types, those between lamellae within a fibril and those between growth arms. The thickness of an intrafibrillar molten area is quite small, of the same magnitude as the lamellae themselves. The interfibrillar molten spaces are generally much larger and provide larger confined domains in which new lamellae may nucleate or grow. For the conditions used in Figure 10, the intrafibrillar molten zones are quite narrow and regular, while the interfibrillar molten zones are much broader, but are somewhat sparsely scattered.

Figure 10 parts b–d relate to the growth of PBS within the PVDF spherulite scaffold. After quickly cooling to 85 °C, PBS starts to grow within the PVDF spherulite scaffold from the top left to the bottom right, filling the remaining molten space. Most of the PBS lamellae grow in the edge-on orientation, but a few grow face-on, and these few face-on crystals cover the underlying

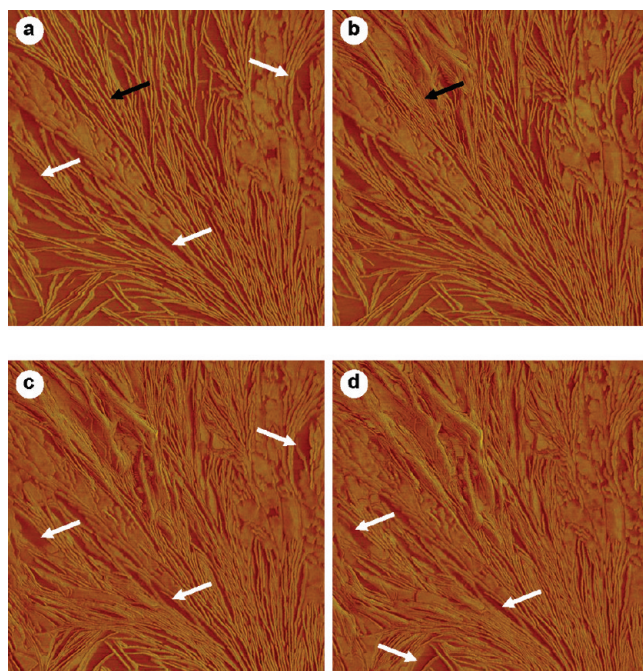


**Figure 10.** AFM phase images of a 50:50 PVDF/PBS blend with the PVDF matrix first crystallized at 140 °C. (a) Crystallization at 130 °C (higher than the  $T_m$  of PBS). (b, c, and d) are the growth process of PBS after cooling to 85 °C. The scanning time for each image is about 3 min, and the interval between two sequential scanning is about 9 min. The scan size is 3  $\mu\text{m}$ .

material, obscuring the dominant edge-on growth process. Nonetheless, there is enough unobsured area to permit a degree of generalization about the main processes. The new PBS edge-on lamellae are seen mostly in the interfibrillar spaces and infrequently in the intrafibrillar (interlamellar) spaces. An example of intrafibrillar crystallization of PBS can be seen, for example, by comparing the places shown in Figure 10a and b indicated by the black arrows. Small-angle X-ray scattering and electron microscopy investigations on other blend systems have shown that in some cases the crystallization of the lower-melting component is dominantly interfibrillar and in other cases intrafibrillar (see ref 21 for a review and references). Moreover, it should be pointed out that the interfibrillar molten pockets in some places are well-interconnected (see top left of Figure 10a), while in other regions are isolated (see bottom left of Figure 10a and also those indicated by the white arrows). With careful inspection, one may find that the PBS crystals are most quickly formed in the relatively open and interconnected interfibrillar regions, seen by comparing the top left regions of Figure 10a and b. By the time of Figure 10d, the crystallization of PBS is nearly complete, but some unconnected interfibrillar molten pockets remain still in the molten state, as indicated by the white arrows in Figure 10d. This clearly demonstrates the hindrance of PVDF crystals on the development of PBS lamellae. In summary, for crystallization of PBS in a 50:50 PVDF/PBS blend at 85 °C within the scaffold of spherulites of PVDF crystallized at 140 °C, the contribution of interlamellar (intrafibrillar) crystallization is minimal, and the contribution of well-connected interfibrillar pockets is greater than that of less well-connected interfibrillar pockets.

Figure 11 shows the *in situ* growth of PBS at 85 °C in a 30:70 blend with PVDF crystallized at the same crystallization temperature,

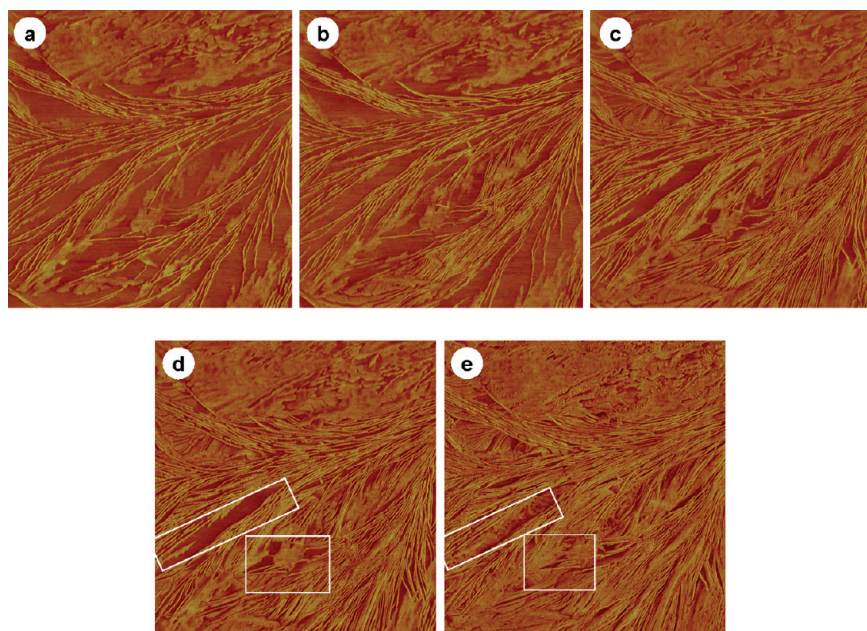


**Figure 11.** AFM phase images of a 30:70 blend with the PVDF matrix first crystallized at 140 °C. (a) Scanning at 130 °C. (b, c, and d) are the growth process of PBS after cooling to 85 °C. (e) Crystallization of PBS corresponding to the rectangle parts of (d) after cooling to much lower temperature (e.g., 50 °C). The time interval between two sequential scans is the same as above. The scan size is 3.0  $\mu\text{m}$ .

that is, 140 °C. As seen in Figure 11a, the morphology prior to the crystallization of PBS is somewhat similar to that of the 50/50 blend; there are well-defined fibrils, separated by interfibrillar pockets of molten polymer. The lamellar organization within the fibrils is nearly as regular as that seen in Figure 10a, but larger molten spaces remain between the fibrils, and the molten pockets are better connected. Therefore, the growth rate of the PBS in this PVDF scaffold, composed of large and interconnected pockets, should be larger compared to the 50:50 blend with PVDF crystallized at the same temperature.

Following completion of PBS crystallization at 85 °C, there are still some remaining interfibrillar molten pockets, as seen in Figure 11c. These pockets crystallize upon lowering the temperature to 50 °C. This can be seen by comparing the rectangle-outlined regions in Figure 11d and e, Figure 11e representing the state at 50 °C. This reflects again the influence of PVDF morphological features on the crystal growth of PBS.

During the crystallization of PBS, we see that the interfibrillar molten spaces are gradually filled with PBS lamellae, as shown in Figure 11c and d. The growth of PBS is nonuniform, and there is no regular growth front; that is, PBS crystallization within each interfibrillar molten pocket seems to nucleate and grow without obvious relation to PBS crystallization in neighboring molten pockets. This certainly cannot be true. The coherent growth front seen in polarized light micrographs shows clearly that indeed a front moves through the PVDF spherulitic scaffold. The evidence shown in the AFM images suggests that the triggering mechanism by which the front is transmitted is subtle and not yet detectable. It is as if the process of propagation entailed the nucleation and growth of PBS lamellae within each pocket, triggered in some as yet unknown manner.

From the AFM observations, it is concluded that the interconnectedness of the adjacent molten pockets is an important factor that determines the intraspherulitic effects of the PVDF on the subsequent crystallization of PBS. Taking this into account, a

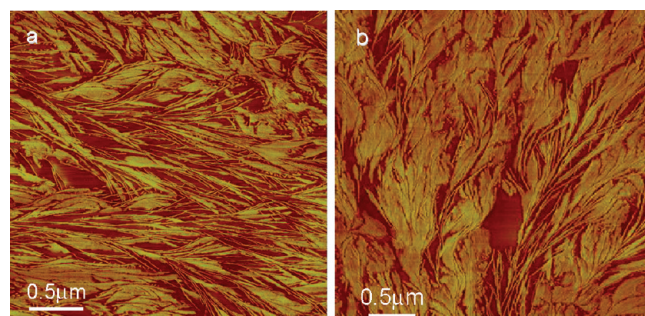


**Figure 12.** AFM phase images of PVDF matrix in the 50:50 blend crystallized at (a) 130 °C and (b) 150 °C, scanning at 130 °C with the PVDF fully crystallized but with no PBS crystallization.

comparison of the morphologies of PVDF in the 50:50 blends crystallized at different temperatures is helpful for explaining the growth rate dependence of PBS on  $T_{\text{c},\text{PVDF}}$ . As presented in Figure 12, at a lower crystallization temperature of PVDF, for example, 130 °C, as shown in Figure 12a, within the PVDF spherulites is an admixture of edge-on and flat-on lamellae coexisting in the scanned area. The lamellar organization is less regular than that seen in Figure 10a (a 50:50 blend with PVDF crystallized at 140 °C), exhibiting a much lower degree of mutual orientation among the edge-on lamellae, relative to that seen in Figure 10a. Fibrils, or stacks of lamellae, are not clearly defined and contain fewer coherently stacked lamellae. Interfibrillar spaces are likewise small and not clearly defined. The result is a morphology in which the largest molten pockets are smaller and less interconnected than the interfibrillar pockets seen for PVDF crystallized at 140 °C (Figure 10a). Therefore, a slower crystal growth is expected. On the other hand, when the PVDF matrix is precrystallized at 150 °C (Figure 12b), there is a larger fraction of face-on, relative to edge-on, PVDF lamellae. The flat-on lamellae

act to occlude the interfibrillar and interlamellar molten pockets below them, which should again result in a more hindered, slower crystal growth of PBS in this less well-connected PVDF matrix. What we have seen then is that the molten within PVDF spherulites formed at 140 °C are better connected than the molten pockets formed at the higher lower temperatures. This must result in a PBS growth kinetic maximum for PVDF crystallization near 140 °C. Consequently, the observed unusual kinetic dependence of PBS in the 50:50 blend on the crystallization temperature of the PVDF appears to derive from the connectedness of the molten PBS pockets.

#### 4. SUMMARY

The crystallization and growth behavior of PBS confined within PVDF spherulites has been studied. It was found that PBS exhibited ellipsoidal crystallization domains within the ring-banded PVDF spherulites formed at relatively high crystallization temperatures, indicating that the orientation of PVDF lamellae affect the growth direction of PBS crystallized domains. In the case of PVDF crystallized at somewhat lower  $T_{c,PVDF}$ , PBS prefers to nucleate at the centers and the boundaries of the PVDF matrix spherulites. As the crystallization temperature of PVDF is decreased still further, more densely nucleated PVDF spherulites are found. In this case, PBS growth domains engulf entire PVDF spherulites as the crystallization front propagates. The front maintains a circular shape, indicating that the rate of propagation of the front averages the rate of growth along various directions within a PVDF spherulite. The kinetic study of the growth of PBS indicates that  $G_{PBS}$  increases with decreasing crystallization temperature and increasing PBS content at a given  $T_{PBS}$ , when the PVDF matrix crystallization temperature is fixed. However, at a given  $T_{PBS}$ , different blends show opposite trends of  $G_{PBS}$  versus  $T_{c,PVDF}$  for  $T_{c,PVDF}$  below 145 °C. Above 145 °C, however,  $G_{PBS}$  for both blends studied decrease with increasing  $T_{c,PVDF}$ . *In situ* AFM observations of the PBS growth process show that PBS growing within PVDF spherulites precrystallized at various temperatures documents details of the growth of PBS crystals within PVDF spherulitic scaffolds. The AFM studies show that the pockets of uncrystallized material differ in size, distribution, and interconnectedness with temperature of PVDF crystallization ( $T_{c,PVDF}$ ). It is found that the interconnectedness of the PBS molten pockets within PVDF spherulites is an important factor in defining the kinetics of PBS crystallization within the spherulitic PVDF scaffolds, which leads to the unusual growth rate variation of PBS in the 50:50 blend with  $T_{c,PVDF}$ . A detailed analysis of the growth rate data may be important for a fully understanding of the crystallization mechanism of PBS in the PVDF matrix and will be performed and presented in another piece of work.

#### ■ ASSOCIATED CONTENT

**5 Supporting Information.** Figures showing the optical micrograph of neat PVDF crystallized at 155 °C, the optical micrograph of PBS crystallized on highly oriented PVDF substrate. This material is available free of charge via the Internet at <http://pubs.acs.org>.

#### ■ AUTHOR INFORMATION

##### Corresponding Author

\*E-mail: [skyan@mail.buct.edu.cn](mailto:skyan@mail.buct.edu.cn) or [schultz@udel.edu](mailto:schultz@udel.edu). Tel.: +86-10-64455928. Fax: +86-10-64455928.

#### ■ ACKNOWLEDGMENT

The financial support of the National Natural Science Foundations of China (No. 50833006, 20974011, and 50973008) and the program of Introducing Talents of Discipline to Universities (B08003) is gratefully acknowledged.

#### ■ REFERENCES

- (1) Jungnickel, B.-J. In *Polymer Crystallization: Observations, Concepts and Interpretations*. *Springer Lecture Notes in Physics*; Sommer, J.-U., Reiter, G., Eds.; Springer-Verlag: Berlin, 2002; Chapter 12, pp 207–238.
- (2) *Polymer Blends Handbook*; Utracki, L. A., Ed.; Springer: Heidelberg, 2003; Vols. 1 and 2.
- (3) *Polymer Blends, Macromolecular Symposia* 142; Pascault, J.-P., Ed.; Wiley: New York, 2003.
- (4) Qiu, Z.; Yan, C. Z.; Lu, J. M.; Yang, W. T.; Ikehara, T.; Nishi, T. *J. Phys. Chem. B* 2007, 11, 2783.
- (5) Qiu, Z.; Yan, C. Z.; Lu, J. M.; Yang, W. T. *Macromolecules* 2007, 40, 5047.
- (6) Liu, J. P.; Jungnickel, B.-J. *J. Polym. Sci., Part B: Polym. Phys.* 2007, 45, 1918.
- (7) Lee, J. C.; Tazawa, H.; Ikehara, T.; Nishi, T. *Polym. J.* 1998, 30, 780.
- (8) Ikehara, T.; Nishi, T. *Polym. J.* 2000, 32, 683.
- (9) Terada, Y.; Ikehara, T.; Nishi, T. *Polym. J.* 2000, 32, 900.
- (10) Hirano, S.; Nishikawa, Y.; Terada, Y.; Ikehara, T.; Nishi, T. *Polym. J.* 2002, 34, 85.
- (11) Ikehara, T.; Nishikawa, Y.; Nishi, T. *Polymer* 2003, 44, 6657.
- (12) Qiu, Z.; Ikehara, T.; Nishi, T. *Macromolecules* 2002, 35, 8251.
- (13) Ikehara, T.; Kimura, H.; Qiu, Z. *Macromolecules* 2005, 38, 5104.
- (14) Liu, L.-Z.; Chu, B.; Penning, J. P.; St. J Manley, R. *Macromolecules* 1997, 30, 4398.
- (15) Penning, J. P.; St. J Manley, R. *Macromolecules* 1996, 29, 84.
- (16) Avella, M.; Martuscelli, E. *Polymer* 1988, 29, 1731.
- (17) Avella, M.; Martuscelli, E.; Greco, P. *Polymer* 1991, 32, 1647.
- (18) Lee, J. C.; Tazawa, H.; Ikehara, T.; Nishi, T. *Polym. J.* 1998, 30, 327.
- (19) Qiu, Z.; Ikehara, T.; Nishi, T. *Polymer* 2003, 44, 2799.
- (20) Qiu, Z.; Fujinami, S.; Komura, M.; Nakajima, K.; Ikehara, T.; Nishi, T. *Polymer* 2004, 45, 4515.
- (21) Schultz, J. M. *Front. Chem. China* 2010, 5, 262.
- (22) Qiu, Z. B.; Yan, C. Z.; Lu, J. M.; Yang, W. T. *Macromolecules* 2007, 40, 5047–5053.
- (23) Ikehara, T.; Kurihara, H.; Kataoka, T. *J. Polym. Sci., Part B: Polym. Phys.* 2009, 47, 539.
- (24) Li, H.; Yan, S. *Macromolecules* 2011, 44, 417–428.
- (25) Lu, J.; Qiu, Z.; Yang, W. *Macromolecules* 2008, 41, 141.
- (26) Galeski, A.; Koenczoel, L.; Piorkowska, E.; Baer, E. *Nature* 1987, 325, 40.
- (27) Galeski, A.; Piorkowska, E.; Koenczoel, L.; Baer, E. *J. Polym. Sci., Polym. Phys. Ed.* 1990, 28, 1171.
- (28) Pawlak, A.; Galeski, A. *J. Polym. Sci., Polym. Phys. Ed.* 1990, 28, 1813.